Asymmetric electron energy sharing in electron-impact double ionization of helium

M. Silenou Mengoue* and H. M. Tetchou Nganso
Centre for Atomic, Molecular Physics and Quantum Optics, Faculty of Science, University of Douala, P.O. Box 8580, Douala, Cameroon
(Received 27 October 2016; published 27 December 2016)

We present the fully fivefold differential cross sections (FDCSs) for $(e, 3e)$ processes in helium within the first Born approximation. The calculation is performed for a coplanar geometry in which the incident electron is fast (∼6 keV), the momentum transfer is small (0.24 a.u.), and for an asymmetric energy sharing between both slow ejected electrons at excess energy of 20 eV. Two cases have been considered: $E_1 = 15$ eV, $E_2 = 5$ eV and $E_1 = 8$ eV, $E_2 = 12$ eV. While waiting for new theoretical and experimental results for confrontations, in particular for asymmetric energy sharing, our results clearly demonstrate that, for the same incident energy, the same momentum transfer and the same excess energy, the $(e, 3e)$ process in helium with asymmetric energy sharing between ejected electrons is more likely than the case with symmetric energy sharing. The two- and three-dimensional representation of the FDCSs covering all possible values of the angle of ejections are presented and discussed. The theoretical cross sections are calculated by using a compact-kernel-integral-equation approach associated with the Jacobi matrix method to calculate a three-body wave function and which leads to a full convergence in terms of the basis size.

DOI: 10.1103/PhysRevA.94.062705

I. INTRODUCTION

The study of the double ionization of atoms by photon or electron impact allows one to gain information on correlated systems. In a kinematically complete $(e, 3e)$ experiment, the particles are detected in coincidence and fivefold differential cross sections are deduced. In the case of two-electron atomic targets, such as helium, one deals in the final state with a pure four-body Coulomb problem which, for high incident energies, can be reduced to a three-body problem from a theoretical point of view. However, even in this case, no analytic exact wave function is known for either the scattering or the bound states. Hence, approximations are made, and $(e, 3e)$ cross sections obtained with different theoretical descriptions of the initial and final states are generally not in agreement either with each other or with high-energy experimental data on helium [1–4]. Several discrete-basis-set methods for the calculation of such processes have recently been developed, including the Coulomb–Sturmian separable expansion method [5,6], the convergent close coupling (CCC) method [1,7], the J-matrix method combined with the Faddeev–Merkuriev equations [8–10], and the generalized Sturmian function (GSF) method [11,12]. In all these approaches, the continuous Hamiltonian spectrum is represented in the context of complete square-integrable bases. Despite the enormous progress made so far in discretization and subsequent numerical solutions of three-body differential and integral equations of Coulomb scattering theory, a number of related problems (one of them is the magnitude of cross sections ...) remain open.

Kinematically completely determined experiments for photo-double ionization of helium have been performed by Bräuning *et al.* [13]. Except for asymmetric electron energy sharings (where discrepancies were found), the corresponding absolute data were in good agreement with the results of various theoretical treatments. In this contribution, we are interested by asymmetric electron energy sharing in He$(e, 3e)$ processes. None of the experimental works cited above have studied this case in particular for ∼6 keV impact energy. Beside the absolute data of Lahmam–Bennani *et al.* [1,2], Dorn *et al.* [3] used 2 keV projectiles and registered collision events with a low-to-intermediate momentum transfer (0.5 a.u.) but undertook only the study of equal-energy sharing. Overall, there is a lack of studies devoted to asymmetric-energy-sharing configurations. The challenging task of this contribution aims to partially fill this gap.

In this paper, we use a compact-kernel-integral-equation approach associated with the Jacobi matrix method to calculate a three-body wave function that describes the double continuum of an atomic two-electron system. This technique has been recently [14] applied to the $(e, 3e)$ experimental kinematic conditions of Refs. [1,2] for symmetric-electron-energy sharing and the fully fivefold differential cross sections (FDCSs) obtained satisfactorily agree both in shape and in magnitude with experiment. In addition, a full convergence in terms of the basis size has been obtained and shown. In the present contribution, we apply this method to the calculation within the first Born approximation of the FDCS for $(e, 3e)$ processes in helium in the small-momentum-transfer regime (0.24 a.u.). The calculation is performed for a coplanar geometry in which the incident electron is fast ∼6 keV and for an asymmetric energy sharing between both slow ejected electrons. Two cases have been considered: $E_1 = 15$ eV, $E_2 = 5$ eV and $E_1 = 8$ eV, $E_2 = 12$ eV. To be more general and predictable in our investigation, we have covered all the possible values of ejected angles θ_1 and θ_2. The two- and three-dimensional representation of the FDCSs corresponding to the two cases mentioned are presented and discussed.

The paper is organized as follows: After this introduction, in the second section, we briefly present the theoretical approach used. The third section is devoted to the results and discussion. The FDCSs are presented for the two asymmetric cases dubbed hereafter case ***A*** ($E_1 = 15$ eV, $E_2 = 5$ eV) and case ***B*** ($E_1 = 8$ eV, $E_2 = 12$ eV). Seen that the excess energy share is the same as the one in Ref. [1], a confrontation curve between symmetric and asymmetric energy sharing is shown. The paper

*smengoue@yahoo.fr

ends in Sec. IV with a brief summary. Atomic units are used throughout.

II. THEORY

The two-electron continuum wave function, i.e., the double continuum wave function with an asymptotic ingoing wave behavior, is a solution of the following Schrödinger equation:

$$\left[E+\frac{1}{2}\triangle_1+\frac{1}{2}\triangle_2+\frac{Z}{r_1}+\frac{Z}{r_2}-\frac{1}{r_{12}}\right]\times\Psi^{(-)}(\mathbf{k}_1,\mathbf{k}_2;\,\mathbf{r}_1,\mathbf{r}_2)=0, \tag{1}$$

where $\mathbf{r}_1$, $\mathbf{r}_2$ are the position vectors of electrons 1 and 2 and $\mathbf{k}_1$, $\mathbf{k}_2$ are their corresponding momentum. $r_{12}=|\mathbf{r}_2-\mathbf{r}_1|$ is the interelectronic distance. Z denotes the charge of the infinitely massive nucleus, the position of which coincides with the origin of the laboratory system. E is the total energy of the two electrons.

Equation (1) is solved in a numerically exact fashion with the approach developed in Ref. [14]. Since the formulation together with relevant computational aspects can be found in our previous work in Ref. [14], only a succinct review is provided hereafter for the sake of providing a self-contained work. Both electrons are identical particles, so we can introduce the new functions $\Psi_i^{(-)}(\mathbf{k}_1,\mathbf{k}_2;\,\mathbf{r}_1,\mathbf{r}_2)\,(i=1,2)$, such that $\Psi^{(-)}=(1/\sqrt{2})[\Psi_1^{(-)}+\Psi_2^{(-)}]$.

Taking into account the exchange symmetry of the solution of Eq. (1), $\Psi^{(-)}(\mathbf{k}_1,\mathbf{k}_2;\,\mathbf{r}_1,\mathbf{r}_2)=g\Psi^{(-)}(\mathbf{k}_1,\mathbf{k}_2;\,\mathbf{r}_2,\mathbf{r}_1)$, where $g=+1$ (-1) for a singlet (triplet) state, we have $\Psi_2^{(-)}(\mathbf{k}_1,\mathbf{k}_2;\,\mathbf{r}_1,\mathbf{r}_2)=g\,\widehat{P}_{12}\Psi_1^{(-)}(\mathbf{k}_1,\mathbf{k}_2;\,\mathbf{r}_1,\mathbf{r}_2)$, so $\Psi^{(-)}=(1/\sqrt{2})[1+g\,\hat{P}_{12}]\Psi_1^{(-)}$. While taking into consideration the method of effective charge, we can now perform a partial-wave decomposition of the wave function $\Psi_1^{(-)}$ and write

$$\begin{aligned}\Psi_1^{(-)}&(\mathbf{k}_1,\mathbf{k}_2;\,\mathbf{r}_1,\mathbf{r}_2)\\&=\frac{2}{\pi}\frac{1}{k_1\,k_2}\sum_{L,M,\lambda_0,l_0}\Big\{\psi^{LM}_{l_0\lambda_0}(\mathbf{r}_1,\mathbf{r}_2;k_1,k_2)\mathcal{Y}^{LM^*}_{l_0\lambda_0}(\widehat{\mathbf{k}}_1,\widehat{\mathbf{k}}_2)\\&\quad\times\theta(k_1-k_2)+g\psi^{LM}_{l_0\lambda_0}(\mathbf{r}_1,\mathbf{r}_2;k_2,k_1)\mathcal{Y}^{LM^*}_{l_0\lambda_0}(\widehat{\mathbf{k}}_2,\widehat{\mathbf{k}}_1)\\&\quad\times\theta(k_2-k_1)\Big\}.\end{aligned} \tag{2}$$

L is the total angular momentum and M its projection on the quantization axis. l_0 and λ_0 are the individual angular momenta of the two electrons. The modified step function θ with $\theta(0)=1/2$ in Eq. (2) is introduced to ensure that, when $k_1>k_2$, the fast ejected electron momentum k_1 is associated with the effective charge $Z-1$ while the slow ejected electron momentum k_2 is associated with the charge Z and inversely. When $k_1=k_2$, the momentum k_1 can be associated with either Z or $Z-1$. $\mathcal{Y}^{LM}_{l_0\lambda_0}(\widehat{\mathbf{p}},\widehat{\mathbf{q}})$ is the bipolar harmonics. The partial-wave function $\psi^{LM}_{l_0\lambda_0}$ in Eq. (2) can be further expanded in a basis of Coulomb–Sturmian functions [15] and bipolar harmonics:

$$\psi^{LM}_{l_0\lambda_0}(\mathbf{r}_1,\mathbf{r}_2)=\sum_{l,\,\lambda,\,n,\,\nu}C^{L(l\lambda)}_{n\nu}(E)\langle\mathbf{r}_1,\mathbf{r}_2|n\,l\,\nu\,\lambda;\;LM\rangle, \tag{3}$$

where the coefficients $C^{L(l\lambda)}_{n\nu}(E)$ are calculated in Ref. [14], and

$$\langle\mathbf{r}_1,\mathbf{r}_2|n\,l\,\nu\,\lambda;\;LM\rangle=\frac{\phi^{\kappa}_{nl}(r_1)}{r_1}\frac{\phi^{\kappa}_{\nu\lambda}(r_2)}{r_2}\mathcal{Y}^{LM}_{l\lambda}(\widehat{\mathbf{r}}_1,\widehat{\mathbf{r}}_2). \tag{4}$$

The Coulomb–Sturmian functions $\phi^{\kappa}_{\nu\lambda}(r)$ form a complete and discrete set of $\mathcal{L}^2$-integrable functions defined as follows:

$$\phi^{\kappa}_{\nu\lambda}(r)=\left[\frac{\kappa(\nu-\lambda-1)!}{\nu(\nu+\lambda)!}\right]^{1/2}(2\kappa r)^{\lambda+1}e^{-\kappa r}L^{2\lambda+1}_{\nu-\lambda-1}(2\kappa r),\quad \nu\geqslant 1+\lambda, \tag{5}$$

where κ is a nonlinear basis parameter. $L^{\alpha}_n(x)$ is a Laguerre polynomial. These functions are known to be orthogonal with the weight $1/r$:

$$\int_0^{\infty}\frac{dr}{r}\phi^{\kappa}_{\nu\lambda}(r)\phi^{\kappa}_{\nu'\lambda}(r)=\frac{\kappa}{\nu}\delta_{\nu\nu'}.$$

The theoretical approach described above to calculate double continuum wave functions is now applied to $(e,3e)$ processes in helium. Here, we consider the case of very high incident energies and small momentum transfer. In this dipole limit, it is expected that a first-order Born treatment is sufficient. The FDCS, which is the most differential cross section, is given by

$$\begin{aligned}\sigma^{(5)}&\equiv\frac{d^5\sigma}{d\Omega_s dE_1 d\Omega_1 dE_2 d\Omega_2}\\&=\frac{4k_sk_1k_2}{k_i}\frac{1}{\mathrm{K}^4}\,|\,\langle\Psi^{(-)}(\mathbf{k}_1,\mathbf{k}_2)|\exp(i\mathbf{K}\cdot\mathbf{r}_1)\\&\quad+\exp(i\mathbf{K}\cdot\mathbf{r}_2)-2|\Psi_0\rangle\,|^2,\end{aligned} \tag{6}$$

where $(E_i,\mathbf{k_i})$, $(E_s,\mathbf{k_s})$, $(E_1,\mathbf{k_1})$, and $(E_2,\mathbf{k_2})$ are the energy and momentum of the incident, scattered, and the two ejected electrons, respectively, and $\mathbf{K}=\mathbf{k_i}-\mathbf{k_s}$ is the momentum transfer. The squared term on the right-hand side of Eq. (6) represents the transition matrix. Its amplitude depends only on three vectors: $\mathbf{k}_1$, $\mathbf{k_2}$, and the momentum transfer $\mathbf{K}$. For small K this amplitude can be Taylor expanded in K, which leads to the optical limit [16]. Within the optical limit, and for first order in K, final and initial states are always orthogonal because only the odd-parity part of the final state contributes to the matrix element, and this odd-parity final state is automatically orthogonal to the even initial state.

Ψ_0 and $\Psi^{(-)}$ are the initial and the final double continuum wave function of helium. The ground-state wave function Ψ_0 is expanded in a basis of the Coulomb–Sturmian functions (5) for the radial coordinates and bipolar harmonics for the angular coordinates [15]:

$$\begin{aligned}\Psi_0(\vec{r}_1,\vec{r}_2)=\sum_{l_1l_2}\sum_{n_1n_2}\gamma^{l_1l_2}_{n_1n_2}\Phi^{l_1l_200}_{n_1n_2}\\\times\mathcal{A}\left(\frac{\phi^{\kappa}_{n_2l_2}(r_2)}{r_2}\mathcal{Y}^{00}_{l_1l_2}(\hat{r}_1,\hat{r}_2)\frac{\phi^{\kappa}_{n_1l_1}(r_1)}{r_1}\right),\end{aligned} \tag{7}$$

where $\Phi^{l_1l_2LM}_{n_1n_2}$ is the expansion coefficient. They are obtained by diagonalizing the atomic Hamiltonian in Eq. (7). The operator $\mathcal{A}$ projects onto either singlet or triplet states in order to ensure the symmetry or antisymmetry of the spatial wave

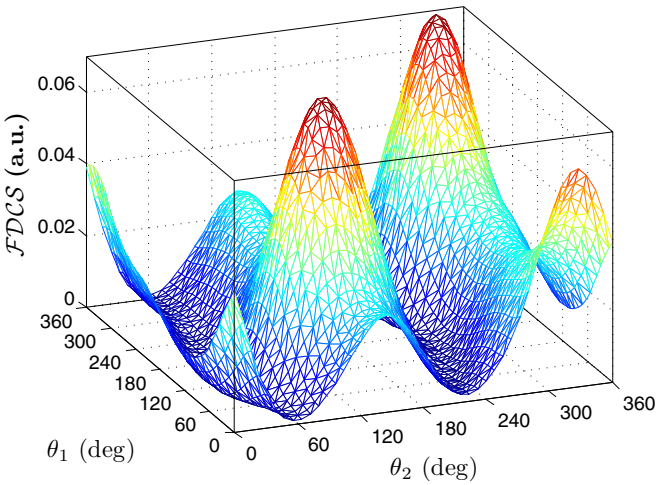

FIG. 1. 3D representation of the FDCS of electron-impact double ionization of helium in the case of asymmetric energy sharing between ejected electrons. The ejected electrons have energies $E_1 = 15$ eV and $E_2 = 5$ eV. The angle of the scattered electron is 0.45° while the angles θ_1 and θ_2 of the ejected electrons vary from 0 to 360°.

function, as required by the Pauli principle. The coefficient $\gamma^{l_1 l_2}_{n_1 n_2} = 1 + (1/\sqrt{2} - 1)\delta^{l_1 l_2}_{n_1 n_2}$ controls the redundancies which, from the exchange of the electrons, may occur in the basis.

III. RESULTS AND DISCUSSION

Calculations of the fully fivefold differential cross section (FDCS) for the He$(e, 3e)$H$_e^{2+}$ reaction on the helium atom were performed. As we mentioned above in Eq. (6), Ψ_0 and $\Psi^{(-)}$ are the initial and the final double continuum wave function of helium. The helium ground-state wave function Ψ_0 is obtained as a result of diagonalization of the matrix of the Hamiltonian of the three-body system. In the present calculation, we put $n_{\max} = \nu_{\max} = 20$ and $l_{\max} = 3$. By choosing the nonlinear parameter $\kappa_0 = 2$, we obtain $E_0 = -2.903\,27$ a.u. for the ground-state energy [17].

The wave function $\Psi^{(-)}$ for the final state of the $(e^-, e^-, \mathrm{H}_e^{2+})$ system is obtained by the method outlined above. In these calculations, it is sufficient to take into account three values (0, 1, and 2) of the total angular momentum L and a maximum value $l_{\max} = 3$ for the individual angular momenta. The number N of Coulomb–Sturmian functions is 50 with the dilation parameter $\kappa = 0.6$. The parameters of the cutoff function are the optimized ones which lead to the convergence of the FDCS in term of basis size in Ref. [14]. They are $\alpha = 5$ and $M = 10$. For the same incident energy $E_0 = 5599$ eV, and the same momentum transfer (0.24 a.u.), we have considered the following two cases:

(1). Case A, in which the ejected electrons energies and effective charge are $E_1 = 15$ eV and $Z_1 = Z - 1$ for the electron 1 and $E_2 = 5$ eV and $Z_2 = Z = 2$ for electron 2.

(2). Case B, in which the ejected electrons energies and effective charges are $E_1 = 8$ eV and $Z_1 = Z = 2$ for the electron 1 and $E_2 = 12$ eV and $Z_2 = Z - 1$ for electron 2.

As mentioned above, no experimental data were found for the He$(e, 3e)$ processes with asymmetric energy sharing between ejected electrons at this incident energy. Thus to be more general and predictable in our investigation, we have covered all the possible values of θ_1 and θ_2. This allows us to plot in two and in three dimensions the curves of the FDCS for cases A and B.

The incident electron energy and the excess energy shared by ejected electrons are the same as in Ref. [1]. Thus we can compare the magnitude of the FDCS in both cases (symmetric and asymmetric electron energy sharing) in order to output the effect of nonequipartition of energy. Within the same spirit state, we will also point out the variation of the minima predicted by the optical limit [16,18] or, more precisely, the one due to Coulomb repulsion.

A. Case A ($E_1 = 15$ eV, $E_2 = 5$ eV)

We start from a general view of the FDCS for the first case in which the incident electron have an energy of 5599 eV while electrons 1 and 2 have energies $E_1 = 15$ eV and $E_2 = 5$ eV,

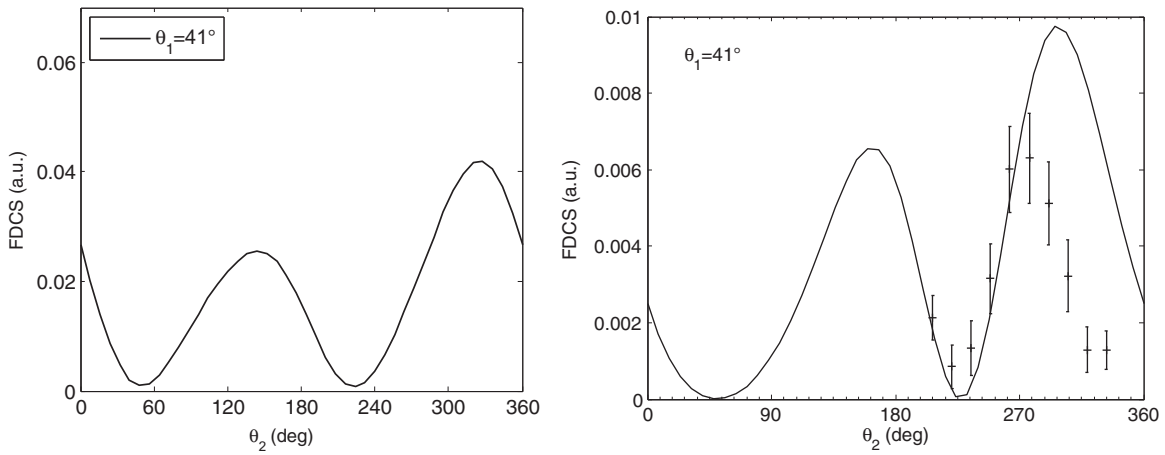

(a) $E_1 = 15$ eV ; $E_2 = 5$ eV (b) $E_1 = E_2 = 10$ eV

FIG. 2. Comparison between (a) the FDCS with asymmetric energy sharing and (b) the FDCS with symmetric energy sharing [14] between ejected electrons. The result is presented for the same excess of energy of the ejected electrons (20 eV) and the same value of the angle $\theta_1 = 41°$, $0° \leqslant \theta_2 \leqslant 360°$. The solid dots with error bars in panel (b) are the absolute experimental data of Lahmam–Bennani [1].

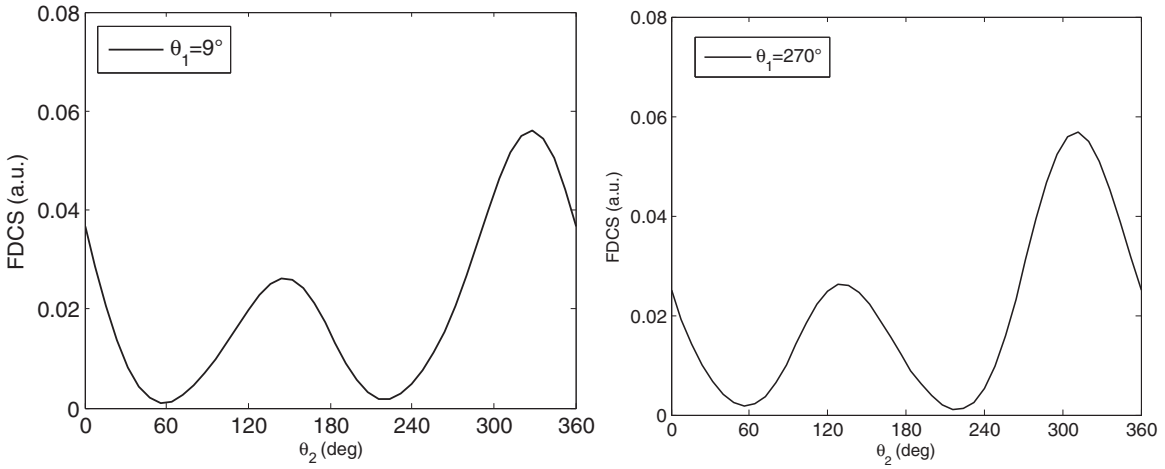

FIG. 3. FDCS (a.u.) of asymmetric electron energy sharing in electron-impact double ionization of helium. The incident energy is $E_0 = 5599$ eV and the energies of the slow ejected electrons are $E_1 = 15$ eV, $E_2 = 5$ eV. The scattering angle θ_s of the fast incident electron is fixed and equal to 0.45° while the angles of the ejected electrons are θ_1 and θ_2. One of these angles, θ_1 is fixed and the other varies.

respectively. The scatter angle is 0.45° and the momentum transfer is equal to 0.24 a.u. Figure 1 is a three-dimensional (3D) representation of the FDCS of electron-impact double ionization of helium in the case of asymmetric energy sharing between ejected electrons (case A) within the first Born approximation (FBA).

In Fig. 2, we compare the FDCS with asymmetric energy sharing [Fig. 2(a)] and the FDCS with symmetric energy sharing [Fig. 2(b)] [14] between ejected electrons. The result is presented for the same excess of energy of 20 eV and the same value of the angle $\theta_1 = 41°$, $0° \leqslant \theta_2 \leqslant 360°$. The solid dots with error bars in Fig. 2(b) are the absolute experimental data of Lahmam–Bennani [1].

As first observation from Fig. 1, one point a two-lobe structure for the FDCS angular distribution. In contrast to the case with symmetric energy sharing in Fig. 2(b), the two lobes are not separated in Fig. 2(a) by zero intensity as predicted by the optical limit. This simply means that the electron-electron interaction is weak in a double-ionization process with $E_1 =$ 15 eV and $E_2 = 5$ eV. The range of intensity of FDCS is also remarkable in the confrontation curves Figs. 2(a) and 2(b). It is clearly seen that, for the same incident energy, the same momentum transfer, and the same excess energy sharing, the $(e, 3e)$ process in helium with asymmetric energy sharing is more plausible than the case with symmetric energy sharing.

In Fig. 3, we present our results of asymmetric electron energy sharing in electron-impact double ionization of helium for two arbitrary values of the angle θ_1 of one of the ejected electron. The first curve, $\theta_1 = 9°$ is for an ejection in the half front plane while the second $\theta_1 = 270°$ is for an ejection in the half rear plane. The two-lobe structure mentioned above is visible. It is clearly seen from Figs. 1–3 that the intensity of the binary lobe which correspond to direction $+\mathbf{K}$ is less than the intensity of the recoil one corresponding to direction $-\mathbf{K}$. Therefore, the residual ion is more implicated in the process when $E_1 > E_2$.

B. Case B ($E_1 = 8$ eV, $E_2 = 12$ eV)

Here we have performed the same theoretical study as above. The individual energies of the ejected electrons are respectively $E_1 = 8$ eV and $E_2 = 12$ eV. The energy of the incident electron remains 5599 eV for a momentum transfer of 0.24 a.u. and a scattered angle equal to $\theta_s = 45°$. We have initially plotted a three-dimensional (3D) curve that then follows the two-dimensional curves. Figure 4 is a 3D representation of the FDCS of electron-impact double ionization of helium in the case of asymmetric energy sharing between ejected electrons (case B) within the FBA.

The first interesting observation from Fig. 4 is the magnitude of the FDCS. They are greater than case A in which the ejected electrons energies were $E_1 = 15$ eV and $E_2 = 5$ eV. The two-lobe structure as well as the approximate zero between lobes predicted in the optical limit are visible. For more detail about these observations, we have plotted in Fig. 5

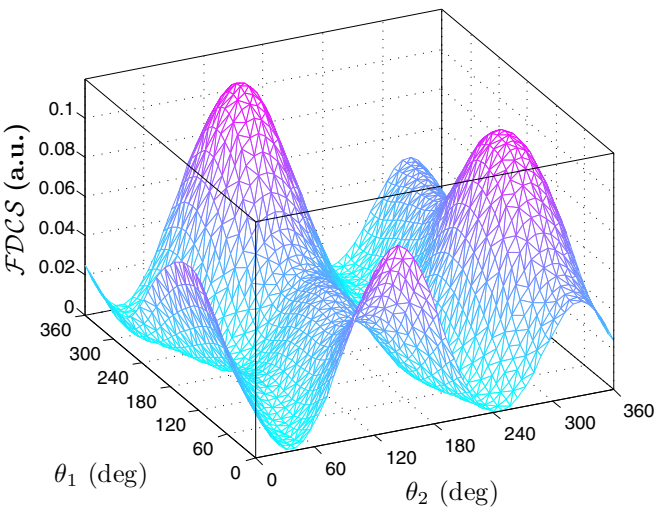

FIG. 4. 3D representation of the FDCS of electron-impact double ionization of helium in the case of asymmetric energy sharing between ejected electrons. The ejected electrons energies are $E_1 = 8$ eV and $E_2 = 12$ eV. The angle of the scattered electron is 0.45° while the angles θ_1 and θ_2 of the ejected electrons vary from 0 to 360°.

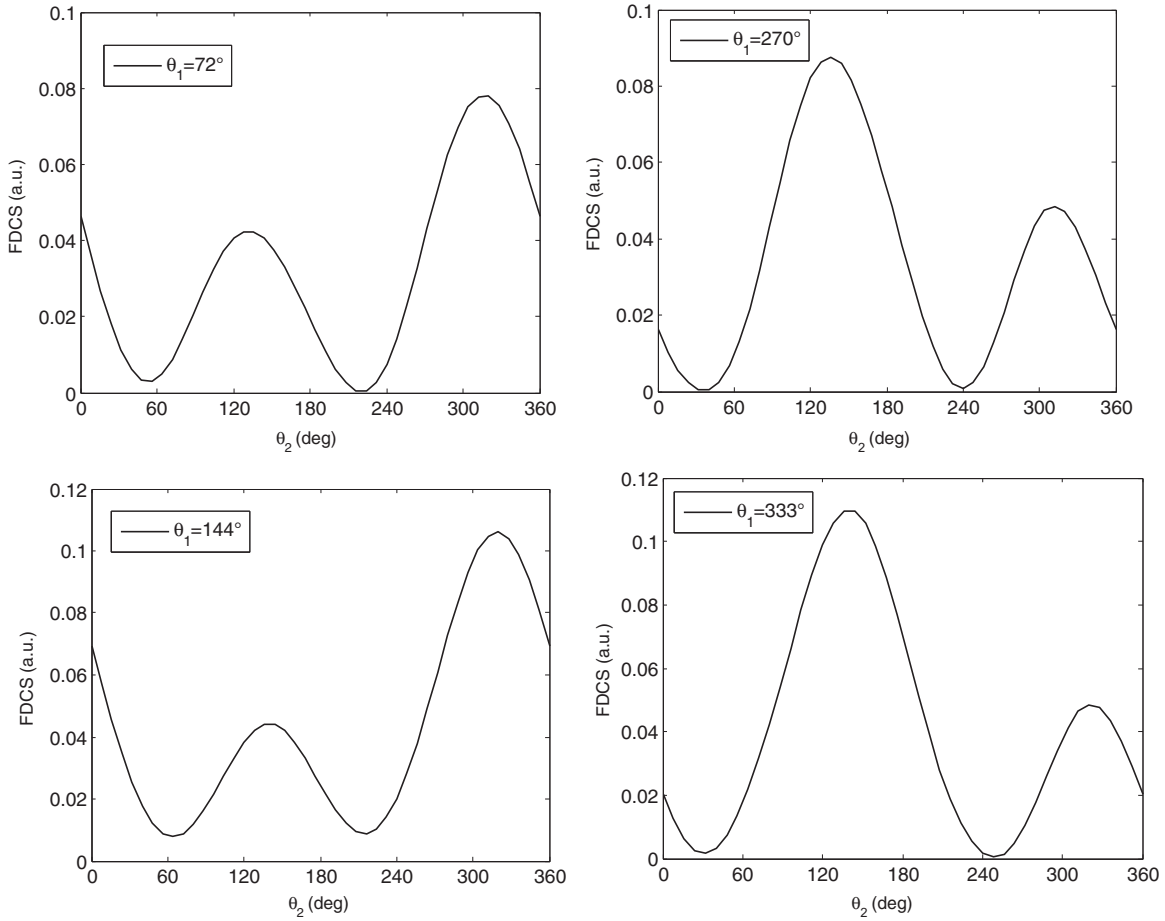

FIG. 5. FDCS (a.u.) of asymmetric electron energy sharing in electron-impact double ionization of helium for $\theta_1 = 72^\circ$, 144°, 270°, and 333°. The incident energy is 5599 eV while the electrons individual energies are $E_1 = 8$ eV, $E_2 = 12$ eV.

the results of the FDCS as a function of the one of the ejected electron angle θ_2, for four arbitrary selected values of the another ejected electron angle θ_1.

From Fig. 5, we notice that, in the two curves $\theta_1 = 72^\circ$ and $\theta_1 = 144^\circ$ for an ejection in the half-front plane, the binary lobes in the direction of $+\mathbf{K}$ are smaller than the recoil ones. The opposite is observed on the two curves $\theta_1 = 270^\circ$ and $\theta_1 = 333^\circ$ for an ejection in the half-rear plane, which means that the residual ion does not participate more actively in the collisional process in this latter case. The positions of the minima at $\hat{k}_1 = \pm\hat{k}_2$ predicted by the dipole limit are violated in case B. In fact, for a fixed momentum transfer K, the dynamical matrix element in Eq. (6) depends very strongly on the scattering geometry, i.e., on k_1 and k_2. This means that, for a fixed K, the optical limit might be approached for certain combination of k_1 and k_2 but violated for other $k_1^{'}$ and $k_2^{'}$.

IV. SUMMARY

In this paper, we present the results of the fully fivefold differential cross section of asymmetric electron energy sharing in electron-impact double ionization of helium by using the approach presented in Ref. [14]. In that approach the wave function is calculated in a way such as the corresponding Lippmann–Schwinger-type equation for the (e^-, e^-, H_e^{2+}) system possess a compact kernel. We performed a first-order Born calculation of the FDCS where we considered a coplanar kinematic that involve a very high incident energy ∼6 keV, a very small momentum transfer of 0.24 a.u., and slow ejected electrons sharing asymmetrically the excess energy of 20 eV. Two cases have been considered: case $\boldsymbol{A}$ ($E_1 = 15$ eV, $E_2 = 5$ eV) and case $\boldsymbol{B}$ ($E_1 = 8$ eV, $E_2 = 12$ eV).

From the theoretical results obtained, it comes out that the magnitude of FDCSs in case B are greater than those in case A. The two- and three-dimensional plots of the FDCSs in both cases A and B showed a two-lobe structure as predicted by the dipole limit. In this optical limit, the positions of the predicted minima were approximately better reproduced in case A than in case B. Let us stress that the minima are just approximated because, in an asymmetry energy sharing, the electron-electron interaction between both ejected electrons is weaker than in a symmetric energy sharing. We also notice that the residual ion is more implicated in the process when $E_1 > E_2$. Finally, Fig. 2 clearly demonstrates that, for the same incident energy, the same momentum transfer and the same excess energy, the $(e, 3e)$ process in helium with asymmetric energy sharing is more likely than the case with symmetric energy sharing. While

waiting for new $(e, 3e)$ experiments, especially for ∼6 keV impact and for asymmetric energy sharing, we are of the opinion that this work could stimulate additional studies.

ACKNOWLEDGMENTS

The authors thank the Université Catholique de Louvain (UCL, Belgium) for providing them with access to the supercomputer of the Consortium des Equipements de Calcul Intensif en Fédération Wallonie Bruxelles (CECI) funded by the Fonds de la Recherche Scientifique de Belgique (F.R.S.-FNRS). The authors are grateful to the Abdus Salam International Centre for Theoretical Physics (ICTP, Trieste, Italy) for its support through the OEA-AC-71 projet. The authors express their gratitude to Professor B. Piraux for warm hospitality at the UCL and the active cooperation between his Laboratory and CEPAMOQ. The authors finally wish to thank Professor Yu. V. Popov and Professor G. Gasaneo for interesting discussions about many aspects of Sturmian functions and three-body Coulomb problems.

[1] A. Kheifets, I. Bray, A. Lahmam-Bennani, A. Duguet, and I. Taouil, J. Phys. B: At., Mol. Opt. Phys. **32**, 5047 (1999).
[2] I. Taouil, A. Lahmam-Bennani, A. Duguet, and L. Avaldi, Phys. Rev. Lett. **81**, 4600 (1998).
[3] A. Dorn, A. Kheifets, C. D. Schröter, B. Najjari, C. Höhr, R. Moshammer, and J. Ullrich, Phys. Rev. Lett. **86**, 3755 (2001).
[4] A. Dorn, A. Kheifets, C. D. Schröter, B. Najjari, C. Höhr, R. Moshammer, and J. Ullrich, Phys. Rev. A **65**, 032709 (2002).
[5] Z. Papp and W. Plessas, Phys. Rev. C **54**, 50 (1996).
[6] Z. Papp, J. Darai, C.-Y. Hu, Z. T. Hlousek, B. Knya, and S. L. Yakovlev, Phys. Rev. A **65**, 032725 (2002).
[7] A. S. Kheifets and I. Bray, Phys. Rev. A **69**, 050701(R) (2004).
[8] S. A. Zaytsev, V. A. Knyr, Yu. V. Popov, and A. Lahmam-Bennani, Phys. Rev. A **75**, 022718 (2007).
[9] V. A. Knyr, S. A. Zaytsev, Yu. V. Popov, and A. Lahmam-Bennani, in *The J-matrix Method: Recent Developments and Selected Applications*, edited by A. Alhaidari, E. J. Heller, H. A. Yamani, and M. S. Abdelmonem (Springer, Dordrecht, 2008).
[10] M. Silenou Mengoue, M. G. Kwato Njock, B. Piraux, Yu. V. Popov, and S. A. Zaytsev, Phys. Rev. A **83**, 052708 (2011).
[11] M. J. Ambrosio, F. D. Colavecchia, D. M. Mitnik, and G. Gasaneo, Phys. Rev. A **91**, 012704 (2015).
[12] G. Gasaneo, D. M. Mitnik, J. M. Randazzo, L. U. Ancarani, and F. D. Colavecchia, Phys. Rev. A **87**, 042707 (2013).
[13] H. Bräuning, R. Dörner, C. L. Cocke, M. H. Prior, B. Krässig, A. S. Kheifets, I. Bray, A. Bräuning-Demian, K. Carnes, S. Dreuil, V. Mergel, P. Richard, J. Ullrich, and H. Schmidt-Böcking, J. Phys. B: At., Mol. Opt. Phys. **31**, 5149 (1998).
[14] M. Silenou Mengoue, Phys. Rev. A **87**, 022701 (2013).
[15] E. Foumouo, G. L. Kamta, G. Edah, and B. Piraux, Phys. Rev. A **74**, 063409 (2006).
[16] A. Lahaman-Bennani, I. Taouil, A. Duguet, M. Lecas, L. Avaldi, and J. Berakdar, Phys. Rev. A **59**, 3548 (1999).
[17] G. W. F. Drake, *Handbook of Atomic, Molecular and Optical Physics* (Springer, New York, 2006).
[18] J. Berakdar, H. Klar, J. Phys. B: At., Mol. Opt. Phys. **26**, 4219 (1993).